PHYSICS OF FLUIDS VOLUME 16, NUMBER 7 JULY 2004

Faxén-like relations for a nonuniform suspension

Kengo Ichiki[a)]
Department of Mechanical Engineering, The Johns Hopkins University, Baltimore, Maryland 21218

Andrea Prosperetti[b)]
Department of Mechanical Engineering, The Johns Hopkins University, Baltimore, Maryland 21218 and Faculty of Applied Physics, Twente Institute of Mechanics and Burgerscentrum, University of Twente, AE 7500 Enschede, The Netherlands

(Received 22 October 2003; accepted 17 February 2004; published online 2 June 2004)

The first part of the paper shows how ensemble averages that correspond to a *prescribed* statistically nonuniform spatial distribution of particles can be evaluated starting from a statistically uniform ensemble. The method consists of attributing to each realization of the uniform ensemble a suitable weight which is explicitly constructed. As an application of this general procedure, in the second part of the paper, the behavior of particles subjected to force or torque in a statistically nonuniform suspension and the behavior of a suspension subjected to a uniform shear are studied. In particular, it is shown how the average translational and angular velocities of the particles with respect to the mixture satisfy Faxén-like relations. Furthermore, it is pointed out that several quantities which vanish in an identical way in the case of a uniform suspension are nonzero in the presence of spatial nonuniformities. © *2004 American Institute of Physics.* [DOI: 10.1063/1.1734951]

I. INTRODUCTION

The construction of a general theory of suspensions and other disperse two-phase flows is an important problem in statistical physics and fluid mechanics that has significant implications for both science and technology.

In view of the limited success of phenomenological approaches, considerable effort has been devoted to the development of such a theory starting from the fundamental microscopic description of fluid–particle and particle–particle interactions. The early analytical studies by Batchelor,[1,2] Brenner,[3–5] Mazur,[6,7] and their co-workers and many others were mostly limited to dilute situations. The advent of powerful numerical simulation techniques, such as those described in Refs. 8–13, opened the way to the study of dense suspensions and the literature contains many papers devoted, on the one hand, to the characterization of dense suspensions in terms of their effective properties such as viscosity[14,15] and hindrance function[16] and, on the other, to the direct simulation of specific flows, such as channel flow.[17–19] In spite of the obvious usefulness of such direct simulations, computational limitations prevent their application to practical flows for which the only possible description is, and will remain for a long time to come, in terms of averaged equations. For this reason, the study of average effective properties such as the effective viscosity and mean hydrodynamic interphase force remains of primary importance.

With very few exceptions that are restricted to the dilute situation,[20,21] all the studies devoted to the derivation of such macroscopic properties have dealt with statistically spatially uniform systems. It is clear that the view of suspension behavior gained in this way is a partial one. For example, in the simple shear flow of a uniform suspension, the velocity of force-free particles is the same as the local volumetric velocity of the mixture and, therefore, the only remaining effective property is the effective viscosity multiplying the rate-of-strain tensor of this mean flow. While, in principle, one could construct a rate-of-strain tensor of the relative motion and a corresponding viscosity,[22] no information on this new quantity can be gained from simulation of a uniform system. The same applies to many other effective properties of a suspension. To be sure, formally, these nonuniformity effects scale as the ratio of the particle radius a to the macroscopic length L, or of the mean interparticle distance $a\phi^{-1/3}$, where ϕ is the particle volume fraction, to L, but this consideration is not sufficient to dismiss them. For example, while in Stokes flow the velocity disturbance generated by a particle extends over a distance proportional to a, the proportionality constant is large so that the corresponding a/L correction is not always negligible. Furthermore, important specific effects of spatial nonuniformity have been identified, such as shear-induced diffusion,[23,24] stratification,[25,26] and others. Fundamentally, this issue is related to the finite size of the particles which is a central aspect of the behavior of dense suspensions.

These considerations have motivated our recent work on statistically nonhomogeneous suspensions.[22,27–29] This paper is a continuation and extension of that work and consists of two parts. In the first part, we show how ensemble averages corresponding to an *arbitrarily prescribed* macroscopic nonuniformity can be calculated. In the second part of the paper, we consider one such simple nonuniformity, a sine wave, and, by ensemble averaging the results of many thousands of direct simulations, derive for a suspension Faxén-like relations analogous to the well-known ones applicable to single particles. It is also argued that, while derivation of the result

[a)]Electronic mail: ichiki@mailaps.org
[b)]Electronic mail: prosperetti@jhu.edu

relies on a specific spatial nonuniformity, the validity of the conclusion is more general and extends to arbitrary situations with weak nonuniformities. Following standard practice (see, e.g., Refs. 10, 15, 30, 31), simulations are conducted in a periodic cell containing randomly arranged particles. The present formulation also confirms the earlier derivation of microscopic quantities, such as the mixture velocity, which was carried out by different means.[29]

In Sec. II, we introduce an ensemble average method which can treat arbitrary nonuniformities. In Sec. III, we show a procedure to evaluate physical quantities for nonuniform suspensions using the nonuniform ensemble average. In Sec. V, the numerical results for linear sinusoidal nonuniformity are shown.

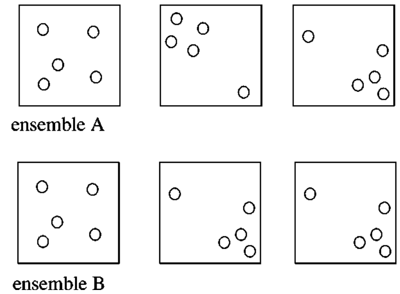

FIG. 1. Sketch of the generation of ensemble averages for spatially statistically nonuniform systems on the basis of a spatially uniform ensemble. Ensemble A is (roughly) uniform, whereas ensemble B has a preferential concentration of particles in the lower right corner. Averages over ensemble B can be calculated by attributing weights of 1, 0, and 2, respectively, to the configurations of ensemble A.

II. NONUNIFORM ENSEMBLE

A widely used procedure to study the bulk properties of an extended (ideally, infinite) suspension is to fill the space with copies of a fundamental cell in which the particles are randomly arranged. The relevant equations are then solved only in the fundamental cell with periodicity boundary conditions.

In this section, we demonstrate how to evaluate ensemble averages for a nonuniform suspension on the basis of a statistically uniform ensemble of random arrangements of particles inside the fundamental cell, thus avoiding the generation of an actual nonuniform ensemble. Using this device, the uniform ensemble can be used to derive the statistical properties of a suspension with built-in, prescribed, spatial nonuniformity.

A. Universal ensemble

Using a procedure which will be explained in Sec. IV C, we construct a statistical ensemble by randomly arranging N_p nonoverlapping equal spherical particles with radius a in a cubic cell of side L.

In principle, this ensemble contains all possible configurations, regular and uniform as well as nonuniform or even heavily biased in the spatial arrangement of the particles. It is evident that, if equal weight is assigned to each configuration, the resulting ensemble averages will correspond to a statistically homogeneous system. However, by giving the configurations unequal weights, this same ensemble can also mimic a spatially nonuniform system. It is for this reason that we refer to the ensemble constructed as ‘‘universal.’’

To illustrate the point by a simple cartoon-like example, Fig. 1 shows two ensembles, A and B, each consisting of three configurations with five particles. Ensemble A (roughly) describes a spatially uniform system, while ensemble B describes a system in which the accumulation of particles in the right lower corner is more likely. Evidently, instead of constructing ensemble B, the same statistical bias can be obtained by assigning weights 1, 0, and 2, respectively, to the configurations in ensemble A. This is obvious. The nontrivial question, to which we now provide an answer, is how to assign the weights in such a way that a *prescribed* spatial nonuniformity can be generated.

More precisely, we consider the following problem: Given a generic quantity $A(\mathcal{C}_i^{N_p})$ pertaining to the i-th realization of an ensemble of N_c configurations $\{\mathcal{C}_1^{N_p},\ldots,\mathcal{C}_{N_c}^{N_p}\}$, each with N_p particles, define its average by

$$\langle A\rangle=\frac{1}{N_c}\sum_{i=1}^{N_c}\mathcal{W}(\mathcal{C}_i^{N_p})A(\mathcal{C}_i^{N_p}),\tag{1}$$

where the $\mathcal{W}(\mathcal{C}_i^{N_p})$ are suitable weights. How should these weights be chosen for the average defined to correspond to a system with prescribed macroscopic nonuniformity in the particle position? Clearly, when all the weights are taken as equal to 1, we have the uniform-ensemble average, denoted by the index 0:

$$\langle A\rangle_0=\frac{1}{N_c}\sum_{i=1}^{N_c}A(\mathcal{C}_i^{N_p}).\tag{2}$$

B. Uniform and nonuniform averages

Each realization $\mathcal{C}_i^{N_p}$ of the ensemble consists of a set of vectors, $\mathbf{x}_i^1$, $\mathbf{x}_i^2,\ldots$, with $\mathbf{x}_i^{N_p}$ denoting the position of the center of particle 1, 2,...,N_p. For the realization $\mathcal{C}_i^{N_p}=\{\mathbf{x}_i^1,\mathbf{x}_i^2,\ldots,\mathbf{x}_i^{N_p}\}$, the (microscopic) number density is defined by

$$n_i(\mathbf{x})=\sum_{\alpha=1}^{N_p}\delta(\mathbf{x}-\mathbf{x}_i^{\alpha}),\tag{3}$$

and can be expanded in a Fourier series:

$$n_i(\mathbf{x})=\sum_{\mathbf{k}}\tilde{n}_i(\mathbf{k})e^{-i\mathbf{k}\cdot\mathbf{x}},\tag{4}$$

with the coefficients given by

$$\tilde{n}_i(\mathbf{k})=\frac{1}{V}\int d\mathbf{x}e^{i\mathbf{k}\cdot\mathbf{x}}n_i(\mathbf{x})=\frac{1}{V}\sum_{\alpha=1}^{N_p}e^{i\mathbf{k}\cdot\mathbf{x}_i^{\alpha}},\tag{5}$$

where $V=L^3$ is the volume of the fundamental cell. The summation in (4) is extended to all $\mathbf{k}$ vectors compatible with the cell. For $\mathbf{k}=\mathbf{0}$ we evidently have

$$\tilde{n}_i(\mathbf{0})=\frac{N_p}{V}=n_0 \tag{6}$$

for all realizations and, therefore,

$$\langle n\rangle_0=n_0 \tag{7}$$

is the volume-averaged particle number density. For nonzero $\mathbf{k}$, we have

$$\langle\tilde{n}(\mathbf{k})\rangle_0=\left\langle\frac{1}{V}\sum_{\alpha=1}^{N_p}e^{i\mathbf{k}\cdot\mathbf{x}_i^\alpha}\right\rangle_0=0. \tag{8}$$

Thus, we can write

$$\langle\tilde{n}(\mathbf{k})\rangle_0=n_0\delta_{\mathbf{k}0}. \tag{9}$$

For $\mathbf{k}\neq 0$, the static structure factor $S(\mathbf{k})$ of the uniform ensemble is related to $\tilde{n}$ by

$$\langle\tilde{n}(-\mathbf{k}')\tilde{n}(\mathbf{k})\rangle_0=\delta_{\mathbf{k}'\mathbf{k}}\frac{N_p}{V^2}S(\mathbf{k}). \tag{10}$$

In order to generate weights for the nonuniform ensemble, we introduce a function $w(\mathbf{x})$ that is regular in the fundamental cell and with the same periodicity, and assign to the i-th realization $\mathcal{C}_i^{N_p}$ the weight $\mathcal{W}(\mathcal{C}_i^{N_p})$ defined by

$$\begin{aligned}\mathcal{W}(\mathcal{C}_i^{N_p})&=\frac{1}{N_p}\sum_{\alpha=1}^{N_p}w(\mathbf{x}_i^\alpha)\\&=\frac{1}{N_p}\int d\mathbf{x}w(\mathbf{x})n_i(\mathbf{x})=\frac{1}{n_0}\sum_{\mathbf{k}}\tilde{w}(\mathbf{k})\tilde{n}_i(-\mathbf{k}).\end{aligned} \tag{11}$$

The relation between the function $w(\mathbf{x})$ and the spatial structure of the ensemble is readily found by calculating the average number density with the above-defined weights. For $\mathbf{k}=\mathbf{0}$ we have

$$\langle\tilde{n}(\mathbf{0})\rangle=n_0\frac{V}{N_p}\sum_{\mathbf{k}}\tilde{w}(\mathbf{k})\langle\tilde{n}(-\mathbf{k})\rangle_0=n_0\tilde{w}(\mathbf{0}), \tag{12}$$

where we use (1) with (6) and (11), from which $\tilde{w}(\mathbf{0})=1$. For $\mathbf{k}\neq\mathbf{0}$,

$$\langle\tilde{n}(\mathbf{k})\rangle=\frac{1}{N_c}\sum_{i=1}^{N_c}\mathcal{W}(\mathcal{C}_i^{N_p})\tilde{n}_i(\mathbf{k})=\tilde{w}(\mathbf{k})\frac{S(\mathbf{k})}{V}, \tag{13}$$

where we use (10). We thus conclude that, if the desired average number density is given by

$$\langle n\rangle(\mathbf{x})\equiv n(\mathbf{x}), \tag{14}$$

we can generate it by assigning to each configuration of the ensemble a weight according to (11), where the function w is given in terms of its Fourier coefficients by

$$\tilde{w}(\mathbf{k})=\frac{V}{S(\mathbf{k})}\tilde{n}(\mathbf{k}), \tag{15}$$

in which $\tilde{n}(\mathbf{k})$ is the Fourier coefficient of the prescribed number density (14).

C. Field and particle quantities

Extending the previous considerations to a generic field quantity $A(\mathbf{x})$, we expand it in a Fourier series as

$$A(\mathbf{x})=\sum_{\mathbf{k}}\tilde{A}(\mathbf{k})e^{-i\mathbf{k}\cdot\mathbf{x}}, \tag{16}$$

where

$$\tilde{A}(\mathbf{k})=\frac{1}{V}\int d\mathbf{x}e^{i\mathbf{k}\cdot\mathbf{x}}A(\mathbf{x}). \tag{17}$$

The nonuniform ensemble average of A with weight $\tilde{w}(\mathbf{k})$ is given by

$$\langle A\rangle(\mathbf{x})=\langle\tilde{A}(\mathbf{0})\rangle_0+\frac{1}{n_0}\sum_{\mathbf{k}\neq\mathbf{0}}\sum_{\mathbf{k}'}\tilde{w}(\mathbf{k}')\langle\tilde{n}(-\mathbf{k}')\tilde{A}(\mathbf{k})\rangle_0e^{-i\mathbf{k}\cdot\mathbf{x}}, \tag{18}$$

where the averages with subscript 0 are taken over the homogeneous ensemble defined in (2). This form is found after observing that, for $\mathbf{k}\neq 0$, $\langle\tilde{n}(-\mathbf{k})\tilde{A}(\mathbf{0})\rangle_0=0$ and $\langle\tilde{A}(\mathbf{k})\rangle_0=0$.

Rather than dealing with complex exponentials, for actual computations it is more convenient to make use of Fourier expansions in a real form. For a generic field quantity $A(\mathbf{x})$ the Fourier representation analogous to (16) is

$$A(\mathbf{x})=\tilde{A}(\mathbf{0})+\sum_{\mathbf{k}>0}\{\tilde{A}^c(\mathbf{k})\cos(\mathbf{k}\cdot\mathbf{x})+\tilde{A}^s(\mathbf{k})\sin(\mathbf{k}\cdot\mathbf{x})\}, \tag{19}$$

where $\mathbf{k}>0$ appended to the summation restricts it to wave numbers all of whose components are positive, and

$$\tilde{A}^c(\mathbf{k})=\frac{2}{V}\int d\mathbf{x}A(\mathbf{x})\cos(\mathbf{k}\cdot\mathbf{x}), \tag{20}$$

$$\tilde{A}^s(\mathbf{k})=\frac{2}{V}\int d\mathbf{x}A(\mathbf{x})\sin(\mathbf{k}\cdot\mathbf{x}). \tag{21}$$

In addition to field variables, the averages of quantities A^α carried by each particle α are also of interest. Examples are the translational and angular velocity, the force multipoles, and others. In order to calculate these averages, we first transform A^α to a field variable by writing

$$A(\mathbf{x})=\sum_{\alpha=1}^{N_p}\delta(\mathbf{x}-\mathbf{x}^\alpha)A^\alpha. \tag{22}$$

The Fourier coefficients are then

$$\tilde{A}^c(\mathbf{k})=\frac{2}{V}\sum_{\alpha=1}^{N_p}A^\alpha\cos(\mathbf{k}\cdot\mathbf{x}^\alpha), \tag{23}$$

$$\tilde{A}^s(\mathbf{k})=\frac{2}{V}\sum_{\alpha=1}^{N_p}A^\alpha\sin(\mathbf{k}\cdot\mathbf{x}^\alpha), \tag{24}$$

and their averages are readily calculated as in (18). After this step, the particle average is calculated from

$$\langle A\rangle^P(\mathbf{x})=\frac{\langle A\rangle(\mathbf{x})}{\langle n\rangle(\mathbf{x})}. \tag{25}$$

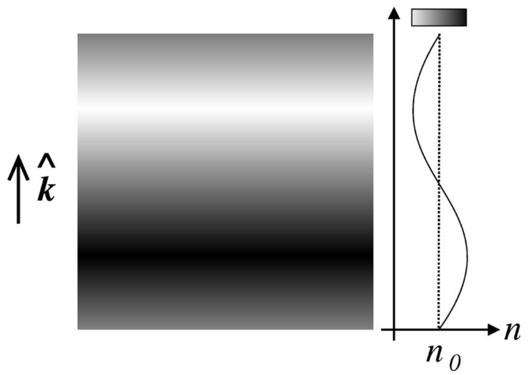

FIG. 2. Example of linear sinusoidal nonuniformity.

The need for normalization by $\langle n\rangle(\mathbf{x})$ is readily proven by considering the special case of $A^\alpha=1$. With this device, we can treat in a unified way both field and particle quantities through their Fourier coefficients $\tilde{A}(\mathbf{k})$.

D. Linear sinusoidal nonuniformity

In applications of the statistical method described in this paper, we limit ourselves to a nonuniform suspension with weak spatial nonuniformity specified by the number density (Fig. 2),

$$n(\mathbf{x})=n_0[1+\epsilon \sin(\mathbf{k}\cdot\mathbf{x})]. \tag{26}$$

It will be argued, however, that the results found in this way extend to general weak nonuniformities. In (26) we take $|\mathbf{k}|$ equal in modulus to the smallest wave number $k_0=2\pi/L$ and oriented in one of the three spatial directions. Henceforth, $\mathbf{k}$ will denote one of these three wave-number vectors. The parameter ϵ is the degree of nonuniformity, and we present results valid to first order in this quantity. In principle, since the Stokes problem that we study is linear, linearization in ϵ enables us to use Fourier superposition to describe weak nonuniformities of any form. It should be noted that, to first order in k included, the volume fraction ϕ has the same spatial dependence[27]

$$\phi(\mathbf{x})=\phi_0[1+\epsilon \sin(\mathbf{k}\cdot\mathbf{x})]+O(k^2), \tag{27}$$

in which $\phi_0=\frac{4}{3}\pi a^3 n_0$.

With this choice of $n(\mathbf{x})$, all the weight coefficients vanish except

$$\tilde{w}(\mathbf{0})=1, \quad \tilde{w}^s(\mathbf{k})=\epsilon n_0\frac{V}{S(\mathbf{k})}. \tag{28}$$

Therefore, the nonuniform ensemble average of the Fourier coefficients $\tilde{A}$ becomes

$$\langle\tilde{A}\rangle=\langle\tilde{A}\rangle_0+\epsilon\langle\tilde{A}\rangle_s, \tag{29}$$

where the nonuniform part $\langle\tilde{A}\rangle_s$ is given by

$$\langle\tilde{A}\rangle_s=\frac{1}{2}\frac{V}{S(k)}\langle\tilde{n}^s(\mathbf{k})\tilde{A}\rangle_0, \tag{30}$$

with, on the basis of (5),

$$\tilde{n}^s(\mathbf{k})=\frac{2}{V}\sum_{\alpha=1}^{N_p}\sin(\mathbf{k}\cdot\mathbf{x}^\alpha). \tag{31}$$

The ensemble average of the Fourier expansion (19) therefore takes the form

$$\langle A\rangle(\mathbf{x})=\langle\tilde{A}(\mathbf{0})\rangle_0+\epsilon[\langle\tilde{A}^c(\mathbf{k})\rangle_s\cos(\mathbf{k}\cdot\mathbf{x}) + \langle\tilde{A}^s(\mathbf{k})\rangle_s\sin(\mathbf{k}\cdot\mathbf{x})], \tag{32}$$

since all other coefficients vanish.

For particle averages, (25) gives, up to $O(\epsilon)$,

$$\langle A\rangle^P(\mathbf{x})=\frac{1}{n_0}\{\langle\tilde{A}(\mathbf{0})\rangle_0+\epsilon[\langle\tilde{A}^c(\mathbf{k})\rangle_s\cos(\mathbf{k}\cdot\mathbf{x}) + (\langle\tilde{A}^s(\mathbf{k})\rangle_s-\langle\tilde{A}(\mathbf{0})\rangle_0)\sin(\mathbf{k}\cdot\mathbf{x})]\}. \tag{33}$$

Equations (32) and (33) show another reason why the introduction of parameter ϵ is useful: The terms multiplied by ϵ originate exclusively from the spatial nonuniformity and therefore, by focusing on them, we are able to identify unambiguously the effect of this nonuniformity even in the presence of the inevitable statistical noise.

III. PARAMETERIZATION

In this paper, we study three kinds of mobility problems for nonuniform suspensions, namely, the flow induced by mobile particles subject to constant force (referred to as the "force problem" in the following), constant torque (the "torque problem"), or shear bulk flow (the "shear problem"). We carry out direct numerical simulations by solving the Stokes equations for each configuration of the ensemble by the method described in Sec. IV. From the results for each realization of the ensemble, we calculate statistical averages according to the relations developed in the previous section.

It is useful to present the results using suitable parameterization, which we now describe. For convenience, we make use of a unified notation which is first introduced in the context of the force problem, and then extended to the other cases.

A. Force problem

For the force problem, i.e., sedimentation, we conduct numerical simulations where the same force $\mathbf{F}_0$ is applied to each particle. The uniform version of this problem is therefore characterized by a single fundamental vector,

$$\mathbf{W}_F=\frac{\mathbf{F}_0}{6\pi\mu a}, \tag{34}$$

with μ the fluid viscosity, and, therefore, any vectorial dependent variable $\mathbf{p}$, such as the mean settling velocity, must take the form

$$\langle\mathbf{p}\rangle=[p]_F^0\mathbf{W}_F, \tag{35}$$

where $[p]_F^0$ is a coefficient calculated numerically by taking the ensemble average of the values of $\mathbf{p}$. Here and in the following we use subscript F for all quantities which refer to the applied force problem.

When we turn to the nonuniform case, in addition to $\mathbf{W}_F$, the wave vector $\mathbf{k}$ that specifies the direction of the nonuniformity is also introduced. Therefore, it must be possible to parameterize the nonuniform part of each vectorial dependent variable as

$$\langle \mathbf{p} \rangle = [p]_F^{\parallel} \mathbf{W}_F^{\parallel} + [p]_F^{\perp} \mathbf{W}_F^{\perp}, \tag{36}$$

where the superscripts $\parallel$ and $\perp$ are based on the direction of unit wave vector $\hat{\mathbf{k}}$ and

$$\mathbf{W}_F^{\parallel} = (\hat{\mathbf{k}}\hat{\mathbf{k}}) \cdot \mathbf{W}_F, \tag{37}$$

$$\mathbf{W}_F^{\perp} = (\mathbf{I} - \hat{\mathbf{k}}\hat{\mathbf{k}}) \cdot \mathbf{W}_F. \tag{38}$$

Clearly $\mathbf{W}_F = \mathbf{W}_F^{\parallel} + \mathbf{W}_F^{\perp}$. The only characteristic pseudovector is

$$a \boldsymbol{\omega}_F^{\perp} = \hat{\mathbf{k}} \times \mathbf{W}_F, \tag{39}$$

which is perpendicular to $\mathbf{k}$; the factor a is included so that $\boldsymbol{\omega}_F^{\perp}$ has the dimensions of angular velocity. Therefore, any pseudovector $\mathbf{q}$ must be parameterized as

$$\mathbf{q} = [q]_F^{\perp} \boldsymbol{\omega}_F^{\perp}. \tag{40}$$

Note that $a\hat{\mathbf{k}} \times \boldsymbol{\omega}_F^{\perp} = -\mathbf{W}_F^{\perp}$, and the parallel component $\boldsymbol{\omega}_F^{\parallel}$ is zero.

B. Torque problem

In the second problem, we apply a constant torque $\mathbf{T}_0$ to each particle and use the subscript T to denote the pertinent quantities. Here, for the uniform case, pseudovectors must be parameterized as

$$\mathbf{q} = [q]_T^0 \boldsymbol{\omega}_T, \tag{41}$$

with

$$\boldsymbol{\omega}_T = \frac{\mathbf{T}_0}{8\pi\mu a^3}. \tag{42}$$

For the nonuniform case we have a single vector,

$$\mathbf{W}_T^{\perp} = a\hat{\mathbf{k}} \times \boldsymbol{\omega}_T, \tag{43}$$

and two pseudovectors,

$$\boldsymbol{\omega}_T^{\parallel} = (\hat{\mathbf{k}} \cdot \boldsymbol{\omega}_T)\hat{\mathbf{k}}, \tag{44}$$

$$\boldsymbol{\omega}_T^{\perp} = (\mathbf{I} - \hat{\mathbf{k}}\hat{\mathbf{k}}) \cdot \boldsymbol{\omega}_T. \tag{45}$$

Note that $\hat{\mathbf{k}} \times \mathbf{W}_T^{\perp} = -a\boldsymbol{\omega}_T^{\perp}$.

C. Shear problem

In the third problem, we apply linear shear flow, so that, even in the uniform case, there is a velocity field imposed given by

$$\mathbf{u}^{\infty}(\mathbf{x}) = \mathbf{E}^{\infty} \cdot \mathbf{x}, \tag{46}$$

where $\mathbf{E}^{\infty}$ is the rate-of-strain tensor of the flow and is symmetric and traceless. The corresponding results will carry an index E. Because we cannot construct any vector or pseudovector from $\mathbf{E}^{\infty}$ only, there cannot be any uniform contribution to vectors $\mathbf{p}$ or pseudovectors $\mathbf{q}$ for the shear problem. In the nonuniform case, one can construct two characteristic vectors,

$$\mathbf{W}_E^{\parallel} = a(\hat{\mathbf{k}}\hat{\mathbf{k}}) \cdot (\mathbf{E}^{\infty} \cdot \hat{\mathbf{k}}), \tag{47}$$

$$\mathbf{W}_E^{\perp} = a(\mathbf{I} - \hat{\mathbf{k}}\hat{\mathbf{k}}) \cdot (\mathbf{E}^{\infty} \cdot \hat{\mathbf{k}}), \tag{48}$$

and one characteristic pseudovector,

$$\boldsymbol{\omega}_F^{\perp} = \hat{\mathbf{k}} \times (\mathbf{E}^{\infty} \cdot \hat{\mathbf{k}}). \tag{49}$$

Note that $\hat{\mathbf{k}} \times \boldsymbol{\omega}_E^{\perp} = -\mathbf{W}_E^{\perp}$.

D. Summary

Because of the linearity of Stokes flow, the results for these three problems can be superposed. Therefore, vectors $\langle \mathbf{p} \rangle$ and pseudovectors $\langle \mathbf{q} \rangle$ are generally parameterized as

$$\langle \mathbf{p} \rangle = [p]_F^0 \mathbf{W}_F + [p]_F^{\parallel} \mathbf{W}_F^{\parallel} + [p]_F^{\perp} \mathbf{W}_F^{\perp} + [p]_T^{\perp} \mathbf{W}_T^{\perp} + [p]_E^{\parallel} \mathbf{W}_E^{\parallel} + [p]_E^{\perp} \mathbf{W}_E^{\perp}, \tag{50}$$

and

$$\langle \mathbf{q} \rangle = [q]_T^0 \boldsymbol{\omega}_T + [q]_F^{\perp} \boldsymbol{\omega}_F^{\perp} + [q]_T^{\parallel} \boldsymbol{\omega}_T^{\parallel} + [q]_T^{\perp} \boldsymbol{\omega}_T^{\perp} + [q]_E^{\perp} \boldsymbol{\omega}_E^{\perp}. \tag{51}$$

IV. NUMERICAL METHOD

We now introduce suitable expressions for the quantities on which we focus in this paper, namely, the average mixture velocity (or volumetric flux), denoted by $\langle \mathbf{u}_m \rangle$, the average mixture angular velocity, $\langle \boldsymbol{\Omega}_m \rangle$, the average particle velocity, $\langle \mathbf{U} \rangle$, and the average particle angular velocity $\langle \boldsymbol{\Omega} \rangle$. The numerical procedures developed earlier and applied to the above quantities are also outlined.

A. Many-body problem

Input to the nonuniform ensemble averaging procedure is the solution of the Stokes many-body problem, which can be expressed in the form of a generalized mobility equation,

$$\begin{bmatrix} \mathbf{U} - \mathbf{U}^{\infty} \\ \boldsymbol{\Omega} - \boldsymbol{\Omega}^{\infty} \\ -\mathbf{E}^{\infty} \\ -\mathcal{U}^{\infty} \end{bmatrix} = \mathcal{M} \cdot \begin{bmatrix} \mathbf{F} \\ \mathbf{T} \\ \mathbf{S} \\ \mathcal{F} \end{bmatrix}, \tag{52}$$

where $\mathbf{U}$ and $\boldsymbol{\Omega}$ are translational and rotational velocities of the particles, and $\mathbf{U}^{\infty}$ and $\boldsymbol{\Omega}^{\infty}$ are defined by

$$\mathbf{U}^{\infty}(\alpha) = \frac{1}{4\pi a^2} \int_{S^{\alpha}} dS(\mathbf{y}) \mathbf{u}^{\infty}, \tag{53}$$

$$\boldsymbol{\Omega}^{\infty}(\alpha) = \frac{1}{4\pi a^2} \int_{S^{\alpha}} dS(\mathbf{y}) \frac{3}{2a^2} (\mathbf{y} - \mathbf{x}^{\alpha}) \times \mathbf{u}^{\infty}(\mathbf{y}). \tag{54}$$

Furthermore, $\mathbf{E}^{\infty}$ and $\mathcal{U}^{\infty}$ are, respectively, the strain tensor and higher order velocity moments of the imposed flow $\mathbf{u}^{\infty}$, $\mathcal{M}$ is the generalized mobility matrix, and $\mathbf{F}$, $\mathbf{T}$, $\mathbf{S}$, and $\mathcal{F}$ are the force, torque, stresslet, and higher order force moments of the particles.[8,32] Detailed definitions are summarized in the Appendix. When $\mathbf{u}^{\infty}$ is itself a Stokes velocity field and, therefore, biharmonic, we have

$$\mathbf{U}^{\infty}(\alpha)=\left(1+\frac{a^2}{6}\nabla^2\right)\mathbf{u}^{\infty}(\mathbf{x}^{\alpha}),\tag{55}$$

$$\boldsymbol{\Omega}^{\infty}(\alpha)=\tfrac{1}{2}\boldsymbol{\nabla}\times\mathbf{u}^{\infty}(\mathbf{x}^{\alpha}).\tag{56}$$

The three problems we study are mobility problems, so **F** and **T** are prescribed. For the imposed flow problem, the quantities $\mathbf{U}^{\infty}$, $\boldsymbol{\Omega}^{\infty}$, $\mathbf{E}^{\infty}$, and $\mathcal{U}^{\infty}$ are also given. Therefore, (52) can be solved, and we obtain **U**, $\boldsymbol{\Omega}$, **S**, and $\mathcal{F}$ for each configuration.

To solve the many-body problem, we use the same numerical code as in previous papers,[22,27] which is based on the method developed by Mo and Sangani.[31] This step is the most time-consuming part of the present method. In the code, $\mathcal{F}$ is expressed by the coefficients of spherical harmonics in Lamb's general solution.[33,34] In order to save time, we use solutions of the many-body problems obtained in Refs. 22 and 27, to which we add new calculations for many other values of both volume fraction ϕ and particle number N_p. For consistency we use the same parameters, taking into account multipoles up to fifth order. In the final processing of the data, however, only multipoles up to the fourth order are included.

For several cases, we also used the Stokesian dynamics method[32] extended to a periodic system (see the Appendix), and have confirmed that the two methods give the same results within the accuracy of multipole truncation.

B. Mixture velocity

Besides particle quantities such as **U** and $\boldsymbol{\Omega}$, we are also interested in $\mathbf{u}_m$, the volumetric flux of the mixture. Tanksley and Prosperetti[29] gave a detailed expression of $\mathbf{u}_m$ in terms of Lamb coefficients; here, we give another expression of $\mathbf{u}_m$.

For a single realization of the ensemble, the mixture velocity $\mathbf{u}_m$ is given by the integral[35,36]

$$\mathbf{u}_m(\mathbf{x})-\mathbf{u}^{\infty}(\mathbf{x})=-\frac{1}{8\pi\mu}\sum_{\alpha=1}^{N_p}\int_{S^{\alpha}}dS(\mathbf{y})\mathbf{J}(\mathbf{x}-\mathbf{y})\cdot\mathbf{f}(\mathbf{y}),\tag{57}$$

where $\mathbf{u}^{\infty}$ is the imposed flow, **J** is the Green's function of the problem, and **f** is the force density at position **y** on the surface of the α-th particle.

Note that $\mathbf{u}_m$ given by (57) is not only defined in the fluid domain, but also inside the particles, where, in fact, it is identical to the rigid-body value,

$$\mathbf{u}_m(\mathbf{x})=\mathbf{U}^{\alpha}+\boldsymbol{\Omega}^{\alpha}\times\mathbf{x},\tag{58}$$

because it is the Stokes solution that satisfies this equation on the particle surface due to the no-slip condition. Therefore, (57) not only gives the fluid velocity in the fluid domain, but also the volumetric flux of the mixture in the whole domain.

In the present theory, we need the Fourier coefficients of the mixture velocity rather than $\mathbf{u}_m(\mathbf{x})$ itself. In this case, we can avoid the complexity of the Ewald summation for periodic boundary conditions and use the expression valid in an infinite volume by modifying wave vector **k** from a continuous to a discrete variable; $\mathbf{J}(\mathbf{r})$ is then the Oseen tensor given by

$$\mathbf{J}(\mathbf{r})=\frac{1}{r}\left(\mathbf{I}+\frac{\mathbf{rr}}{r^2}\right).\tag{59}$$

This is the same procedure as that for the analysis of a periodic system used by Ladd[10] and applied to an infinite system in Ref. 7. Upon using the convolution relation in (57), the Fourier coefficient of the relative velocity $(\mathbf{u}_m-\mathbf{u}^{\infty})$ is given by

$$(\tilde{u}_m)_i(\mathbf{k})=\frac{1}{\mu}\frac{1}{k^2}\left(\delta_{ij}-\frac{k_ik_j}{k^2}\right)\sum_{n=0}^{\infty}\frac{i^nk^n_{k\ldots}}{n!}\tilde{\mathcal{F}}^{(n)}_{j,k\ldots}(\mathbf{k}),\tag{60}$$

where $\tilde{\mathcal{F}}(\mathbf{k})$ is the Fourier coefficient of the force moment $\mathcal{F}$. In real form, the cosine and sine coefficients are

$$(\tilde{u}^c_m)_i(\mathbf{k})=\frac{1}{\mu}\frac{1}{k^2}\left(\delta_{ij}-\frac{k_ik_j}{k^2}\right)\sum_{n=0}^{\infty}(-)^n\left[\frac{k^{2n}_{k\ldots}}{(2n)!}\tilde{\mathcal{F}}^{c(2n)}_{j,k\ldots}(\mathbf{k})-\frac{k^{2n+1}_{k\ldots}}{(2n+1)!}\tilde{\mathcal{F}}^{s(2n+1)}_{j,k\ldots}(\mathbf{k})\right],\tag{61}$$

$$(\tilde{u}^s_m)_i(\mathbf{k})=\frac{1}{\mu}\frac{1}{k^2}\left(\delta_{ij}-\frac{k_ik_j}{k^2}\right)\sum_{n=0}^{\infty}(-)^n\left[\frac{k^{2n}_{k\ldots}}{(2n)!}\tilde{\mathcal{F}}^{s(2n)}_{j,k\ldots}(\mathbf{k})+\frac{k^{2n+1}_{k\ldots}}{(2n+1)!}\tilde{\mathcal{F}}^{c(2n+1)}_{j,k\ldots}(\mathbf{k})\right],\tag{62}$$

where $\tilde{\mathcal{F}}^c(\mathbf{k})$ and $\tilde{\mathcal{F}}^s(\mathbf{k})$ are the cosine and sine coefficients of the force moment, respectively. Equation (60) is equivalent to (8.2) in the paper by Tanksley and Prosperetti.[29]

Note that the coefficient with $\mathbf{k}=\mathbf{0}$ should be dropped in order for the velocity to be nonsingular.[30,37] This specifies the frame of reference as the volume average of the mixture velocity in the fundamental cell is then zero. This is the physical meaning of Batchelor's renormalization.[1]

C. Ensembles

Our interest lies in quantities which correspond to large (ideally infinite) systems, for which $k\to 0$. For each value of ϕ, therefore, it is necessary to construct ensembles that correspond to different values of k so as to be able to calculate this limit. This requires considering ensembles with different numbers of particles N_p as

$$ka=\frac{2\pi a}{L}=\left(\frac{6\pi^2\phi}{N_p}\right)^{1/3}.\tag{63}$$

For ϕ between 1% and 50%, we construct ensembles of between 256 and 2048 configurations with 10–160 particles. Statistical errors in the ensemble averages (2) decrease rather slowly as $1/\sqrt{N_c}$. Considerations of computational time force us to strike a compromise between the number of configurations and the residual statistical error, especially for large numbers of particles. Table I shows the number of configurations we use in the different ensembles.

The ensembles are constructed as follows. For volume fractions less than 50%, we start by randomly arranging the particles in the cell making sure that no overlap occurs, and subject them to a random walk, displacing each one of them taking care to avoid overlaps at each step. After $100N_p$ steps

TABLE I. Number of configurations in the ensemble used in the simulations.

No. of particles, N_p	No. of configurations, N_c
10–16	2048
17–79	1024
80–150	512
160	256

per particle, we store the resultant configuration as a member of the ensemble. The initial configuration is regenerated every time. For ϕ=50%, we start by arranging the N_p particles in a regular array and execute $1000N_p$ random steps after which we store the resulting configuration. This configuration is used as the starting condition for generating the next one. By repeating this procedure, we construct ensembles of N_c configurations.

The static structure factor for hard spheres in infinite space is isotropic and is approximated by the analytical solution of the Percus–Yevick (PY) integral equation[38–40] as

$$S_{\mathrm{PY}}(k)=[1-n_0\tilde{c}(2ka)]^{-1}, \tag{64}$$

where n_0 is the number density, and $\tilde{c}(2ka)$ is the Fourier transform of the direct (isotropic) correlation function given by

$$\begin{aligned}\tilde{c}(X)=-\frac{32\pi a^3}{X^3}\Bigg[&\alpha(\sin X-X\cos X)\\&+\frac{\beta}{X}\{2X\sin X-(X^2-2)\cos X-2\}\\&+\frac{\gamma}{X^3}\{(4X^3-24X)\sin X\\&-(X^4-12X^2+24)\cos X+24\}\Bigg],\end{aligned} \tag{65}$$

where $X=2ka$, and

$$\alpha(\phi)=\frac{(1+2\phi)^2}{(1-\phi)^4}, \tag{66}$$

$$\beta(\phi)=-6\phi\frac{(1+\frac{1}{2}\phi)^2}{(1-\phi)^4}, \tag{67}$$

$$\gamma(\phi)=\frac{\phi}{2}\frac{(1+2\phi)^2}{(1-\phi)^4}. \tag{68}$$

Figure 3 shows a comparison between $S_{\mathrm{PY}}(k)$ and the structure factor $S(k)$ for our ensembles for a volume fraction of 15%. We calculate this quantity according to

$$S(k)=\frac{V^2}{N_p}\langle\tilde{n}(\mathbf{k})\tilde{n}(-\mathbf{k})\rangle_0, \tag{69}$$

considering not only $k=2\pi/L$, but also the higher modes, $\sqrt{2}k$, $\sqrt{3}k$, $2k$, and so on. For each wave vector, the point plotted in Fig. 3 is the average over all different directions of the wave vector. This result shows that, although our ensembles are not strictly isotropic, they give rise to a structure factor that is essentially indistinguishable from the Percus–Yevick distribution in infinite space in the wave vectors range greater than $2\pi/L$. In particular, one may therefore expect that the linear sinusoidal nonuniformity with the smallest wave number k is not affected by the periodicity.

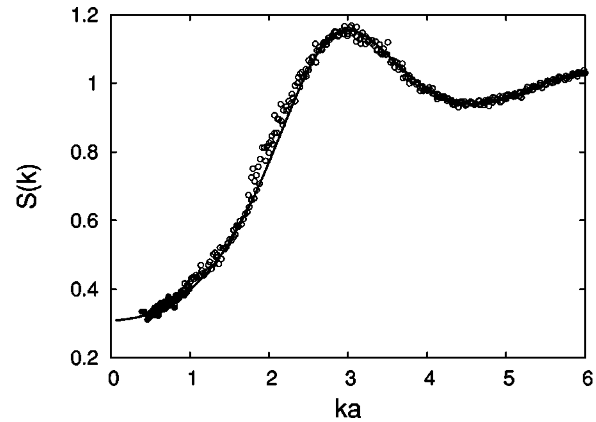

FIG. 3. Comparison between the structure factor given by the Percus–Yevick solution $S_{\mathrm{PY}}(k)$ in (64) (solid line) and $S(k)$ numerically calculated from (69) from the configurations used in the present work for ϕ=0.15. The closed circles are calculated with $k=2\pi/L$, and the open circles are with higher spatial modes.

For all our ensembles, Fig. 4 shows the unscaled nonuniform averages of $\tilde{n}^s(\mathbf{k})$ for the case of linear sinusoidal nonuniformity. According to (30), this quantity is defined by

$$S_s(k)=\frac{V^2}{2N_p}\langle[\tilde{n}^s(\mathbf{k})]^2\rangle_0. \tag{70}$$

Every point represents an ensemble average for given values of ϕ and N_p. A comparison of Fig. 4 with Fig. 3 in a previous paper,[27] shows that, while some results for volume fractions ϕ=0.15, 0.25, and 0.35 have been reused as mentioned before, many more ensembles have been added since then. Note that the universal ensemble is translationally invariant, so that the average $\langle(\tilde{n}^c)^2\rangle_0$ is equal to $\langle(\tilde{n}^s)^2\rangle_0$ within statistical accuracy. Therefore, $S_s(k)$ in (70) is equal to $S(k)$ in

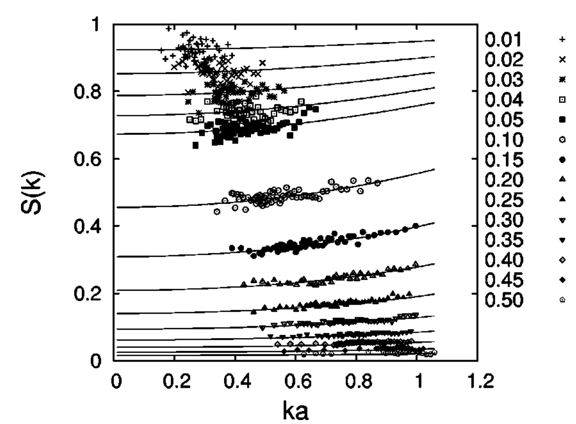

FIG. 4. Structure factor $S_s(k)$ calculated according to (70) for the smallest wave number for each cell of all ensembles used in this study with volume fraction ϕ between 0.01 and 0.50 and particle number N_p between 10 and 160. The lines are the Percus–Yevick solution $S_{\mathrm{PY}}(k)$ in (64) for each volume fraction.

(69). In Fig. 4, we also plot $S_{\mathrm{PY}}(k)$ for reference. This shows that the relative error of $S_s(k)$ from $S_{\mathrm{PY}}(k)$ is independent of ϕ and around 6–8%.

In the calculations that follow, we use this numerically computed $S_s(k)$ as the structure factor for the definition of the nonuniform probability weights in (28).

D. Averaging and parameterization

Here we show how to evaluate the nonuniform ensemble averages with the universal ensembles for each one of the quantities defined above.

1. Field quantities

The Fourier coefficients of the mixture velocity defined by (61) and (62) are averaged according to (29) for each ensemble. Since the coefficient with $\mathbf{k}=\mathbf{0}$ has been dropped, there is no uniform part and, since the mixture is incompressible as a whole,

$$\nabla\cdot\mathbf{u}_m=0, \tag{71}$$

as is obvious from (60). This implies that the parallel component of the nonuniform part of $\mathbf{u}_m$ should be zero. The numerical results also indicate that the cosine coefficient of the nonuniform parts for the force problem and the sine coefficients for torque and shear problems are less than 10% relative to the nonzero coefficients at most. This is of the order of statistical error which may be expected, and we therefore assume they vanish. If we retain only the nonzero terms in the notation in Sec. IV C, we then have

$$\langle\tilde{\mathbf{u}}_m^s(\mathbf{k})\rangle_s=[u_m]_F^{\perp}\mathbf{W}_F^{\perp}, \tag{72}$$

$$\langle\tilde{\mathbf{u}}_m^c(\mathbf{k})\rangle_s=[u_m]_T^{\perp}\mathbf{W}_T^{\perp}, \tag{73}$$

$$\langle\tilde{\mathbf{u}}_m^c(\mathbf{k})\rangle_s=[u_m]_E^{\perp}\mathbf{W}_E^{\perp}, \tag{74}$$

from which

$$\begin{aligned}\langle\mathbf{u}_m-\mathbf{u}^{\infty}\rangle(\mathbf{x})=&\,\epsilon\sin(\mathbf{k}\cdot\mathbf{x})[u_m]_F^{\perp}\mathbf{W}_F^{\perp}\\&+\epsilon\cos(\mathbf{k}\cdot\mathbf{x})[u_m]_T^{\perp}\mathbf{W}_T^{\perp}\\&+\epsilon\cos(\mathbf{k}\cdot\mathbf{x})[u_m]_E^{\perp}\mathbf{W}_E^{\perp}.\end{aligned} \tag{75}$$

The three parameters denoted by square brackets in the parameterizations (72)–(74) are the building blocks for the analysis of nonuniform suspensions given in the next section.

The angular velocity of the mixture, $\mathbf{\Omega}_m$, is

$$\mathbf{\Omega}_m=\tfrac{1}{2}\nabla\times\mathbf{u}_m. \tag{76}$$

Substituting (75), we have

$$\begin{aligned}\left\langle\mathbf{\Omega}_m-\frac{1}{2}\nabla\times\mathbf{u}^{\infty}\right\rangle(\mathbf{x})=&\,\epsilon\cos(\mathbf{k}\cdot\mathbf{x})\frac{k}{2}[u_m]_F^{\perp}\boldsymbol{\omega}_F^{\perp}\\&+\epsilon\sin(\mathbf{k}\cdot\mathbf{x})\frac{k}{2}[u_m]_T^{\perp}\boldsymbol{\omega}_T^{\perp}\\&-\epsilon\sin(\mathbf{k}\cdot\mathbf{x})\frac{k}{2}[u_m]_E^{\perp}\boldsymbol{\omega}_E^{\perp}.\end{aligned} \tag{77}$$

2. Particle quantities

In order to calculate the average of the particle velocity $\mathbf{U}$ for each configuration, we find its Fourier coefficients $\tilde{\mathbf{U}}(\mathbf{0})$, $\tilde{\mathbf{U}}^c$, and $\tilde{\mathbf{U}}^s$ according to (23) and (24), and average them over the configurations to find $\langle\tilde{\mathbf{U}}(\mathbf{0})\rangle_0$, $\langle\tilde{\mathbf{U}}^c\rangle_s$, and $\langle\tilde{\mathbf{U}}^s\rangle_s$. From the numerical results, the uniform parts for the torque and shear problems, the cosine coefficient of the nonuniform part for the force problem, and the sine coefficients for the torque and shear problems vanish. Using parameterizations in the form of (50), we then have

$$\begin{aligned}\langle\mathbf{U}-\mathbf{U}^{\infty}\rangle^P(\mathbf{x})=&\,[U]_F^0\mathbf{W}_F+\epsilon\sin(\mathbf{k}\cdot\mathbf{x})([U]_F^{\parallel}\mathbf{W}_F^{\parallel}\\&+[U]_F^{\perp}\mathbf{W}_F^{\perp})+\epsilon\cos(\mathbf{k}\cdot\mathbf{x})[U]_T^{\perp}\mathbf{W}_T^{\perp}\\&+\epsilon\cos(\mathbf{k}\cdot\mathbf{x})([U]_E^{\parallel}\mathbf{W}_E^{\parallel}+[U]_E^{\perp}\mathbf{W}_E^{\perp}).\end{aligned} \tag{78}$$

In a similar way, for the particle angular velocity $\mathbf{\Omega}$, we have

$$\begin{aligned}\langle\mathbf{\Omega}-\mathbf{\Omega}^{\infty}\rangle^P(\mathbf{x})=&\,[\Omega]_T^0\mathbf{W}_T+\epsilon\cos(\mathbf{k}\cdot\mathbf{x})[\Omega]_F^{\perp}\boldsymbol{\omega}_F^{\perp}\\&+\epsilon\sin(\mathbf{k}\cdot\mathbf{x})([\Omega]_T^{\parallel}\boldsymbol{\omega}_T^{\parallel}+[\Omega]_T^{\perp}\boldsymbol{\omega}_T^{\perp})\\&+\epsilon\sin(\mathbf{k}\cdot\mathbf{x})[\Omega]_E^{\perp}\boldsymbol{\omega}_E^{\perp}.\end{aligned} \tag{79}$$

Note that $\langle\mathbf{U}^{\infty}\rangle^P$ and $\langle\mathbf{\Omega}^{\infty}\rangle^P$ are the particle averages of the moments of the imposed velocity defined in (53) and in (54).

3. Slip velocities

The translational slip velocity $\langle\mathbf{u}_{\Delta}\rangle$ is the average translational velocity of the particles relative to the mixture,

$$\langle\mathbf{u}_{\Delta}\rangle=\langle\mathbf{U}-\mathbf{U}^{\infty}\rangle^P-\langle\mathbf{u}_m-\mathbf{u}^{\infty}\rangle. \tag{80}$$

Upon inserting expression (55) for $\mathbf{U}^{\infty}(\alpha)$ in (22) and then in (25) to calculate $\langle\mathbf{U}^{\infty}\rangle^P$, because of the presence of the factor $\delta(\mathbf{x}-\mathbf{x}^{\alpha})$, we simply find

$$\langle\mathbf{U}^{\infty}\rangle^P=\left(1+\frac{a^2}{6}\nabla^2\right)\mathbf{u}^{\infty}(\mathbf{x}). \tag{81}$$

Furthermore, in the three cases studied in this paper, $\mathbf{u}^{\infty}(\mathbf{x})$ is either a constant or a linear function of $\mathbf{x}$ so the second term can be dropped with the result,

$$\langle\mathbf{u}_{\Delta}\rangle=\langle\mathbf{U}\rangle^P-\langle\mathbf{u}_m\rangle. \tag{82}$$

From parameterization of the particle velocity in (78) and of the mixture velocity in (75), we have

$$\begin{aligned}\langle\mathbf{u}_{\Delta}\rangle(\mathbf{x})=&\,[u_{\Delta}]_F^0\mathbf{W}_F+\epsilon\sin(\mathbf{k}\cdot\mathbf{x})([u_{\Delta}]_F^{\parallel}\mathbf{W}_F^{\parallel}+[u_{\Delta}]_F^{\perp}\mathbf{W}_F^{\perp})\\&+\epsilon\cos(\mathbf{k}\cdot\mathbf{x})[u_{\Delta}]_T^{\perp}\mathbf{W}_T^{\perp}\\&+\epsilon\cos(\mathbf{k}\cdot\mathbf{x})([u_{\Delta}]_E^{\parallel}\mathbf{W}_E^{\parallel}+[u_{\Delta}]_E^{\perp}\mathbf{W}_E^{\perp}),\end{aligned} \tag{83}$$

where

$$[u_{\Delta}]_F^0=[U]_F^0, \tag{84}$$

$$[u_{\Delta}]_F^{\parallel}=[U]_F^{\parallel}, \tag{85}$$

$$[u_{\Delta}]_F^{\perp}=[U]_F^{\perp}-[u_m]_F^{\perp}, \tag{86}$$

$$[u_{\Delta}]_T^{\perp}=[U]_T^{\perp}-[u_m]_T^{\perp}, \tag{87}$$

$$[u_\Delta]_E^\parallel = [U]_E^\parallel, \tag{88}$$

$$[u_\Delta]_E^\perp = [U]_E^\perp - [u_m]_E^\perp. \tag{89}$$

The slip angular velocity $\mathbf{\Omega}_\Delta$ is defined in a similar way by

$$\langle \mathbf{\Omega}_\Delta \rangle = \langle \mathbf{\Omega} - \mathbf{\Omega}^\infty \rangle^P - \langle \mathbf{\Omega}_m - \tfrac{1}{2} \nabla \times \mathbf{u}^\infty \rangle, \tag{90}$$

which, in the present case, using the same argument as before, becomes

$$\langle \mathbf{\Omega}_\Delta \rangle = \langle \mathbf{\Omega} \rangle^P - \langle \mathbf{\Omega}_m \rangle. \tag{91}$$

From the parameterization of the angular particle velocity in (79) and of the angular mixture velocity in (77),

$$\begin{aligned} \langle \mathbf{\Omega}_\Delta \rangle(\mathbf{x}) = {} & [\Omega_\Delta]_T^0 \mathbf{W}_T + \epsilon \cos(\mathbf{k}\cdot\mathbf{x}) [\Omega_\Delta]_F^\perp \boldsymbol{\omega}_F^\perp \\ & + \epsilon \sin(\mathbf{k}\cdot\mathbf{x}) ([\Omega_\Delta]_T^\parallel \boldsymbol{\omega}_T^\parallel + [\Omega_\Delta]_T^\perp \boldsymbol{\omega}_T^\perp) \\ & + \epsilon \sin(\mathbf{k}\cdot\mathbf{x}) [\Omega_\Delta]_E^\perp \boldsymbol{\omega}_E^\perp, \end{aligned} \tag{92}$$

where

$$[\Omega_\Delta]_F^\perp = [\Omega]_F^\perp - \frac{k}{2} [u_m]_F^\perp, \tag{93}$$

$$[\Omega_\Delta]_T^0 = [\Omega]_T^0, \tag{94}$$

$$[\Omega_\Delta]_T^\parallel = [\Omega]_T^\parallel, \tag{95}$$

$$[\Omega_\Delta]_T^\perp = [\Omega]_T^\perp - \frac{k}{2} [u_m]_T^\perp, \tag{96}$$

$$[\Omega_\Delta]_E^\perp = [\Omega]_E^\perp + \frac{k}{2} [u_m]_E^\perp. \tag{97}$$

V. RESULTS

We now present and discuss the results of the multiparticle simulations in light of the framework established earlier. We focus on the slip velocity $\langle \mathbf{u}_\Delta \rangle$, the mixture velocity $\langle \mathbf{u}_m - \mathbf{u}^\infty \rangle$, and the slip angular velocity $\langle \mathbf{\Omega}_\Delta \rangle$. These quantities are parameterized as in (83), (75), and (92), respectively, and we will examine the numerical coefficients in these parameterizations denoted by square brackets. These coefficients depend on both the wave vector k and the volume fraction ϕ.

A. Velocities for the force problem

We start by considering the velocities in the force problem.

Figure 5 shows, for different volume fractions between 1% and 50%, straight-line fits to the coefficients of the parameterization of the uniform part of $\langle \mathbf{U} - \mathbf{U}^\infty \rangle^P$:

$$[U]_F^0(k,\phi) = A^{[U]_F^0} + k B^{[U]_F^0}. \tag{98}$$

The fitting is done by least squares. The error with which (98) approximates the numerical results is smaller than the symbols used to graph $A^{[U]_F^0}$ and $B^{[U]_F^0}$ in Fig. 6. The constant term $A^{[U]_F^0}$ is the hindrance function for sedimentation, $U(\phi)$:

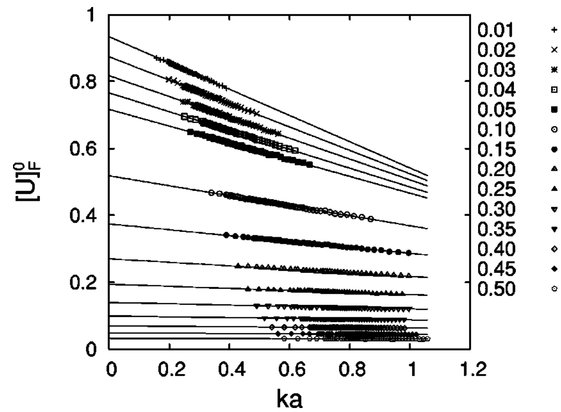

FIG. 5. Uniform part $[U]_F^0$ of the particle velocity for the force problem as a function of k. The points are the numerically calculated ensemble averages and the lines least-squares fits. For this problem, $[U]_F^0$ is equal to the uniform part $[u_\Delta]_F^0$ of the slip velocity.

$$A^{[U]_F^0} = \lim_{k\to 0} [U]_F^0 = U(\phi). \tag{99}$$

Therefore, $A^{[U]_F^0}$ is the sedimentation velocity extrapolated to infinite cell size. As Fig. 6 shows, it is well fitted by

$$U(\phi) = (1-\phi)^{6.55 - 3.4\phi}. \tag{100}$$

Note that our numerical solution is affected by truncation of the multipole expansion because we solve the many-body problems including multipoles only up to fifth order.

The coefficient $B(\phi)$ reflects the effect of the periodicity[10,15,31] which arises from the difference between the sedimentation velocities of random and regular arrays.[41] Several heuristic arguments have been proposed which have led to a relation between B and μ_r, the effective viscosity of the suspension normalized by the fluid viscosity. Mo and Sangani[31] proposed a relation which, in our notation, is

$$B^{[U]_F^0} = - \frac{1.7601}{(6\pi^2)^{1/3}} \frac{S(0)}{\mu_r}, \tag{101}$$

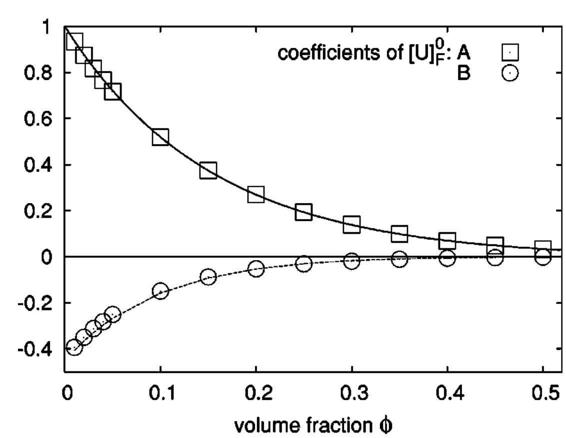

FIG. 6. Coefficients A and B of the linear fit (98) to $[U]_F^0$ as functions of volume fraction ϕ. A coincides with the hindrance function $U(\phi)$ in (99) and B is the effect of the periodicity of the system. Solid and dashed lines are fits (100) for A and the model (101) for B, respectively.

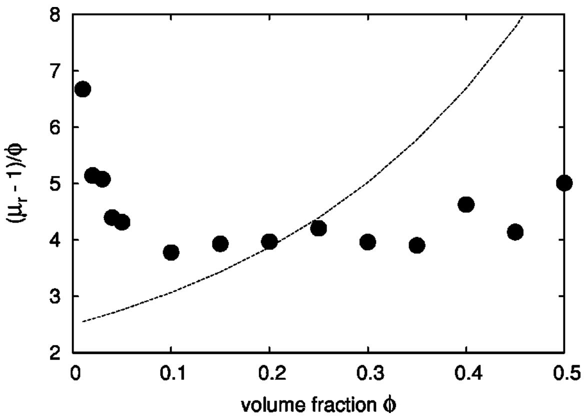

FIG. 7. Comparison of $(\mu_r - 1)/\phi$ calculated directly by averaging the stresslets for the uniform shear problem (line) and from the suggestion (101) given in Ref. 31.

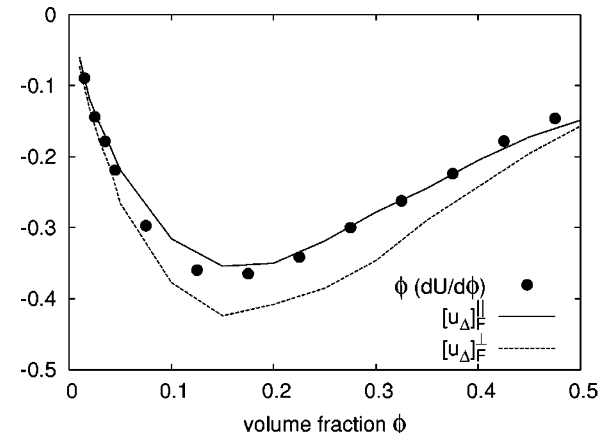

FIG. 8. Comparison of $\phi(\mathrm{d}U/\mathrm{d}\phi)$, $[u_\Delta]_F^{\parallel}$, and $[u_\Delta]_F^{\perp}$ for a nonuniform suspension. The three quantities should coincide if the relation between the force on the particles and the slip velocity did not contain a Faxén-type correction.

in which $S(0)$ is the structure factor for $k=0$. This is also plotted by the dashed line in Fig. 6, where μ_r is evaluated from the uniform shear problem as the average stresslets in the standard way.[10,15,31] Although the model (101) captures the qualitative behavior of B, there is a significant difference between $(\mu_r-1)/\phi$ calculated directly and the value deduced from (101). To better illustrate this difference, Fig. 7 shows $(\mu_r-1)/\phi$ calculated from (101) which, in the dilute limit, should tend toward the Einstein coefficient 5/2 which multiplies the $O(\phi)$ term of μ_r. A similar difference can be observed in Fig. 6 of our previous paper.[27] These results suggest that the relationship between μ_r and $B^{[U]_F^0}$ is more complex than (101) would imply.

The coefficients for the nonuniform parts of $\langle \mathbf{U}-\mathbf{U}^\infty\rangle^P$ and $\langle \mathbf{u}_m - \mathbf{u}^\infty\rangle$ can be fitted as

$$[U]_F^{\parallel} = A^{[U]_F^{\parallel}} + kB^{[U]_F^{\parallel}}, \tag{102}$$

$$[U]_F^{\perp} = \frac{1}{k^2} D^{[U]_F^{\perp}} + A^{[U]_F^{\perp}} + kB^{[U]_F^{\perp}}, \tag{103}$$

$$[u_m]_F^{\perp} = \frac{1}{k^2} D^{[u_m]_F^{\perp}} + A^{[u_m]_F^{\perp}} + kB^{[u_m]_F^{\perp}}. \tag{104}$$

For $k\to 0$, we encounter in terms D of the perpendicular components the same divergence found in Ref. 27. This arises from the lowest order multipole in (60). As noted in Ref. 27, this divergence is physical in that it is due to the fact that, as $k\to 0$, the width (and therefore the weight) of the heavier and lighter bands of the mixture increases, while the shear force which retards their fall does not. These two diverging terms are found to be equal within our numerical accuracy and therefore cancel out upon forming the perpendicular component of the slip velocity, which is therefore given by

$$[u_\Delta]_F^{\perp} = A^{[u_\Delta]_F^{\perp}} + kB^{[u_\Delta]_F^{\perp}}. \tag{105}$$

The coefficients $A^{[u_\Delta]_F^{\perp}}$ and $B^{[u_\Delta]_F^{\perp}}$ are calculated by fitting a linear k dependence to the difference (86).

In order to understand these results, the simplest hypothesis is that the slip velocity is given by the hindrance function evaluated at the local volume fraction. For the linear sinusoidal nonuniformity (27), we would then have

$$U(\phi) = U(\phi_0) + \phi_0 \frac{\mathrm{d}U}{\mathrm{d}\phi}\epsilon \sin(\mathbf{k}\cdot\mathbf{x}). \tag{106}$$

Figure 8 shows $[u_\Delta]_F^{\parallel}$, $[u_\Delta]_F^{\perp}$, and $\phi(\mathrm{d}U/\mathrm{d}\phi)$, where the derivative of the hindrance function is evaluated by numerical differentiation of the results for $[u_\Delta]_F^0$. We see that the simple hypothesis works quite well for the parallel component, but not for the perpendicular one.

To address this difference, it is useful to remember Faxén's law for a single particle,

$$\frac{\mathbf{F}^\alpha}{6\pi\mu a} = \mathbf{U}^\alpha - \left(1 + \frac{a^2}{6}\nabla^2\right)\mathbf{u}'(\mathbf{x}^\alpha), \tag{107}$$

where $\mathbf{u}'$ is the velocity field except for the contribution of particle α. It is reasonable to expect a similar contribution in the present case. Since the mixture velocity $\mathbf{u}_m$ only has a perpendicular component, this contribution would vanish for the parallel one, which would account for the good fit of $[u_\Delta]_F^{\parallel}$ and (106).

We thus introduce a coefficient, $C(\phi;k)$, by

$$U(\phi)\frac{\mathbf{F}_0}{6\pi\mu a} = \langle \mathbf{u}_\Delta\rangle - C(\phi;k)a^2\nabla^2\langle \mathbf{u}_m\rangle. \tag{108}$$

Physically, this equation represents an extension of Faxén's law (107) and of the dilute-limit theory by Geigenmüller and Mazur[42] to the finite volume fraction. By extrapolating to large system size, from the previous results, we find

$$C(\phi) = \lim_{k\to 0} \frac{1}{k^2 a^2 [u_m]_F^{\perp}} ([u_\Delta]_F^{\parallel} - [u_\Delta]_F^{\perp}). \tag{109}$$

Figure 9 shows the values of $C(\phi)$ calculated from this expression together with the reference value of 1/6 suggested by Faxén's law (107). The bars indicate the error in fitting of the least-squares procedure. Convergence is poor at low volume fractions where, due to the increased available phase-space volume, a large number of configurations is necessary

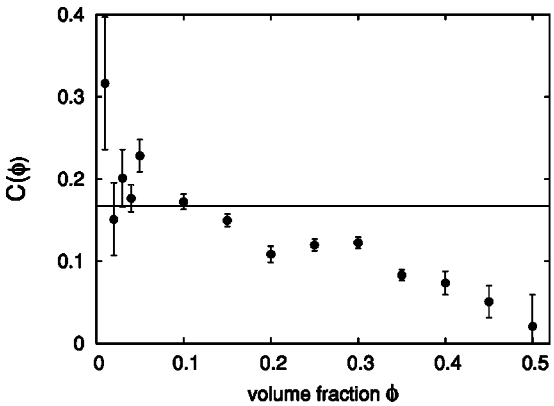

FIG. 9. Coefficient $C(\phi)$ of the Faxén-type correction of the relation between force on the particles and the slip velocity defined in (109). The line is the dilute-limit value 1/6. The fitting error bars are also shown.

for good statistical averaging. At high volume fractions, the error is possibly related to truncation of the multipole expansion. Nevertheless, we find general consistency between our results and (107). It should be stressed that, since $C(\phi)$ is independent of k, by superposition and linearity, the result (108) holds not only for the special form (26) of $n(\mathbf{x})$ but, to order $(a/L)^2$, for any other weak nonuniformity as well.

The Faxén term in Eq. (108) was also studied in our previous paper,[22] where Fig. 10 is, in the present notation, $C(\phi)/U(\phi)$. The present results are consistent with the earlier ones except for the last point in the latter corresponding to $\phi=0.35$. Due to the smaller number of simulations conducted for that earlier study, it is likely that that point is erroneous.

In conclusion, we have found that the averages of the slip velocity are given by

$$[u_\Delta]_F^0 = U(\phi), \tag{110}$$

$$[u_\Delta]_F^{\parallel} = \phi\frac{\mathrm{d}U}{\mathrm{d}\phi}, \tag{111}$$

$$[u_\Delta]_F^{\perp} + C(\phi)k^2[u_m]_F^{\perp} = \phi\frac{\mathrm{d}U}{\mathrm{d}\phi}. \tag{112}$$

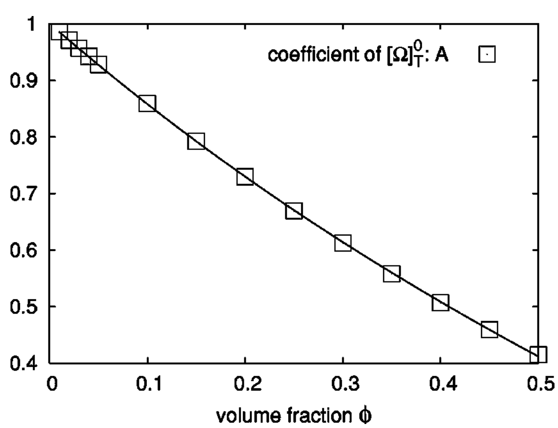

FIG. 10. Hindrance function for rotation $A=\Omega(\phi)$ as a function of the volume fraction.

Feuillebois[20] studied the sedimentation of a dilute suspension that exhibited sinusoidal as well as step-like nonuniformities by taking only two-body interactions into account. In the dilute limit, his results are consistent with the present ones.[27]

B. Angular velocities for the torque problem

For fixed ϕ, the uniform part of the particle angular velocity has essentially no k dependence and is well fitted by a constant,

$$[\Omega]_T^0(k,\phi) = A^{[\Omega]_T^0} = \Omega(\phi), \tag{113}$$

where $\Omega(\phi)$ is the hindrance function for the torque problem. Figure 10 shows $\Omega(\phi)$, which is fitted well by

$$\Omega(\phi) = (1-\phi)^{1.50-0.41\phi}. \tag{114}$$

The nonuniform parts of Ω can be fitted by

$$[\Omega]_T^{\parallel} = A^{[\Omega]_T^{\parallel}} + k^2 C^{[\Omega]_T^{\parallel}}, \tag{115}$$

$$[\Omega]_T^{\perp} = A^{[\Omega]_T^{\perp}} + k^2 C^{[\Omega]_T^{\perp}}. \tag{116}$$

As expected, there is no diverging term here. The contribution of the mixture to the angular velocity Ω_m is

$$[\Omega_m]_T^{\perp} = \frac{k}{2}[u_m]_T^{\perp} = \frac{k^2}{2}\left(\frac{D^{[u_m]_T^{\perp}}}{k^2} + A^{[u_m]_T^{\perp}}\right). \tag{117}$$

The leading terms of Ω and Ω_m are now different and there is no cancellation in the calculation of the slip angular velocity, which is

$$[\Omega_\Delta]_T^{\perp} = A^{[\Omega_\Delta]_T^{\perp}} + k^2 C^{[\Omega_\Delta]_T^{\perp}}. \tag{118}$$

If the local slip angular velocity were only dependent on the local value of the rotational hindrance function, one would expect that

$$\Omega(\phi)\mathbf{T}_0 = 8\pi\mu a^3\langle\mathbf{\Omega}_\Delta\rangle, \tag{119}$$

where

$$\Omega(\phi) = \Omega(\phi_0) + \phi_0\frac{d\Omega}{d\phi}\epsilon\sin(\mathbf{k}\cdot\mathbf{x}), \tag{120}$$

so that

$$[\Omega_\Delta]_T^0 = \Omega(\phi), \tag{121}$$

$$[\Omega_\Delta]_T^{\parallel} = [\Omega_\Delta]_T^{\perp} = \phi\frac{\mathrm{d}\Omega}{\mathrm{d}\phi}, \tag{122}$$

which is tested numerically in Fig. 11. Unlike the force case, the numerical results evidently support the conjecture (119), which conforms with the conventional Faxén law for torque on a single particle. The same argument presented before in connection with (108) can also be used to conclude that (119) holds to order $(a/L)^2$ for any weak spatial nonuniformity.

C. Further examples of the effect of nonuniformity

For uniform suspensions, the slip velocity under applied torque, the slip angular velocity for sedimentation, and both

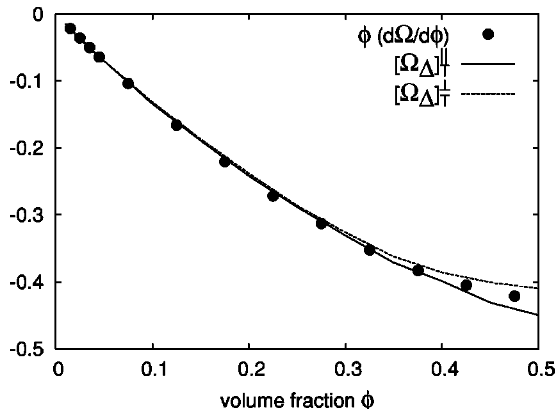

FIG. 11. Comparison of $\phi(\mathrm{d}\Omega/\mathrm{d}\phi)$, $[\Omega_\Delta]^{\parallel}_T$, and $[\Omega_\Delta]^{\perp}_T$ in a nonuniform suspension. The very close similarity among the three quantities implies that the mean torque is directly related to the slip angular velocity without a Faxén-type correction.

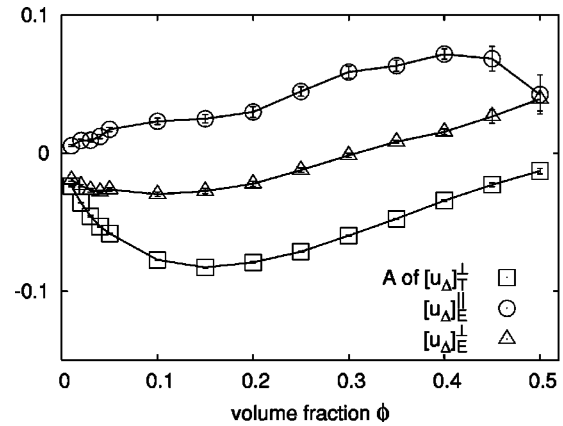

FIG. 12. Coefficient A of the linear term in k in fits of the numerical results for $[u_\Delta]^{\perp}_T$, $[u_\Delta]^{\parallel}_E$, and $[u_\Delta]^{\perp}_E$ for the nonuniform case. Note that, while these quantities would all vanish for a uniform suspension, they are clearly nonzero in the presence of nonuniformity. The fitting error bars are also shown.

slip and slip-angular velocities for imposed shear all vanish. The situation is different in the presence of spatial nonuniformities as we now show.

The computed average velocities for the torque problem can be fitted as

$$[U]^{\perp}_T = k\left(\frac{1}{k^2}D^{[U]^{\perp}_T} + A^{[U]^{\perp}_T}\right), \tag{123}$$

$$[u_m]^{\perp}_T = k\left(\frac{1}{k^2}D^{[u_m]^{\perp}_T} + A^{[u_m]^{\perp}_T}\right). \tag{124}$$

It is shown analytically in Ref. 27 that

$$\lim_{\phi\to 0} D^{[u_m]^{\perp}_T} = 3\phi. \tag{125}$$

Similar to the force problem, the diverging terms of U and u_m are identical, and the leading term of the slip velocity is $O(k)$

$$[u_\Delta]^{\perp}_T = kA^{[u_\Delta]^{\perp}_T}. \tag{126}$$

The coefficient $A^{[u_\Delta]^{\perp}_T}$ is shown by squares in Fig. 12. The error bars inscribed in the symbols give an idea of the fitting error for this quantity. $A^{[u_\Delta]^{\perp}_T}$ is found to be rather small, but systematically nonzero.

For the shear problem, the parallel component of U can be fitted as

$$[U]^{\parallel}_E = kA^{[U]^{\parallel}_E}, \tag{127}$$

and the perpendicular components of U and u_m as

$$[U]^{\perp}_E = k\left(\frac{1}{k^2}D^{[U]^{\perp}_E} + A^{[U]^{\perp}_E}\right), \tag{128}$$

$$[u_m]^{\perp}_E = k\left(\frac{1}{k^2}D^{[u_m]^{\perp}_E} + A^{[u_m]^{\perp}_E}\right), \tag{129}$$

where, for $D^{[u_m]^{\perp}_E}$ Ref. 27 shows that

$$\lim_{\phi\to 0} D^{[u_m]^{\perp}_E} = 5\phi. \tag{130}$$

The diverging terms again cancel upon forming the slip velocity and the leading term of this quantity is $O(k)$,

$$[u_\Delta]^{\perp}_E = kA^{[u_\Delta]^{\perp}_E}. \tag{131}$$

The A coefficients of the parallel and perpendicular components are also shown in Fig. 12 by circles and triangles, respectively. The fitting error bars are inscribed in the symbols. Again, both of these quantities are clearly nonzero.

The average angular velocity coefficients in the force problem can be fitted as

$$[\Omega]^{\perp}_F = k\left(\frac{D^{[\Omega]^{\perp}_F}}{k^2} + A^{[\Omega]^{\perp}_F} + kB^{[\Omega]^{\perp}_F}\right), \tag{132}$$

$$[\Omega_m]^{\perp}_F = \frac{k}{2}\left(\frac{D^{[u_m]^{\perp}_F}}{k^2} + A^{[u_m]^{\perp}_F} + kB^{[u_m]^{\perp}_F}\right), \tag{133}$$

where we have diverging terms which, again, are equal, so that the leading order of the slip angular velocity is $O(k)$,

$$[\Omega_\Delta]^{\perp}_F = k(A^{[\Omega_\Delta]^{\perp}_F} + kB^{[\Omega_\Delta]^{\perp}_F}). \tag{134}$$

The circles in Fig. 13 show $A^{[\Omega_\Delta]^{\perp}_F}$ with the fitting error bars.

The corresponding results for the shear problem take the form

$$[\Omega]^{\perp}_E = k^2\left(\frac{D^{[\Omega]^{\perp}_F}}{k^2} + A^{[\Omega]^{\perp}_F}\right), \tag{135}$$

$$[\Omega_m]^{\perp}_E = -\frac{k}{2}\left(\frac{D^{[u_m]^{\perp}_E}}{k^2} + A^{[u_m]^{\perp}_E}\right), \tag{136}$$

with identical diverging terms so that the leading order of the slip angular velocity is $O(k^2)$,

$$[\Omega_\Delta]^{\perp}_E = k^2A^{[\Omega_\Delta]^{\perp}_E}. \tag{137}$$

Figure 13 shows this A coefficient with the fitting error bars.

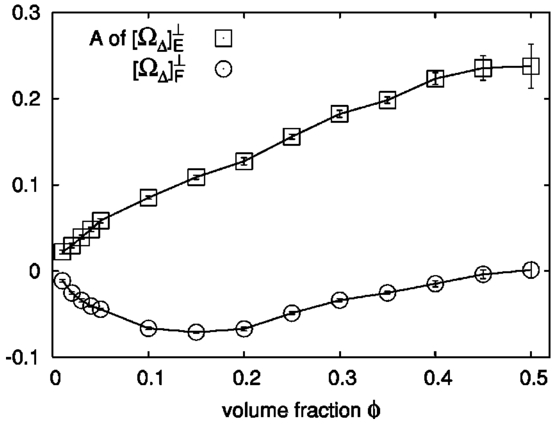

FIG. 13. Coefficient A of the linear term in k in fits of the numerical results for $[\Omega_\Delta]_F^\perp$ and $[\Omega_\Delta]_E^\perp$ for the nonuniform case. While these quantities would all vanish for a uniform suspension, they are clearly nonzero in the presence of nonuniformity. The fitting error bars are also shown.

These results show that, for nonuniform suspensions, the slip velocity $\langle \mathbf{u}_\Delta \rangle$ is nonzero even when no force acts on the particles, and the slip angular velocity $\langle \mathbf{\Omega}_\Delta \rangle$ is nonzero even in the absence of torque. This behavior is quite different from that encountered in the case of uniform suspensions and it suggests that uniform suspension simulations can only give a partial view of the general behavior of a suspension. In particular, characterization of nonuniform suspensions requires the introduction of additional ''effective properties'' (e.g., the Faxén coefficient) with respect to those sufficient to describe a uniform suspension. This issue has been partially addressed in Ref. 22 and will be pursued further in future work.

VI. CONCLUSIONS

In the first part of this paper we have shown how averages that correspond to a spatially nonuniform statistical ensemble can be calculated on the basis of a uniform one. The method consists in attributing to each realization of the uniform ensemble a suitable weight, which is constructed explicitly starting from an arbitrarily prescribed macroscopic particle number density distribution.

We have applied this general theory to the simple case of weak sinusoidal nonuniformity of the number density distribution of equal spheres in a viscous suspension for three mobility problems: sedimentation, the applied torque, and imposed bulk shear flow. In spite of the special form of the nonuniformity, we have shown that the results are valid in general to second order in the ratio $(a/L)^2$, where a is the particle radius and L the macroscopic length scale.

We have found that, in a nonuniform suspension, the average slip angular velocity, i.e., the relative angular velocity between the particles and the mixture, can be calculated by simply evaluating the hindrance function for rotation corresponding to the local concentration, as in Eq. (119):

$$\langle \mathbf{\Omega} \rangle^P - \frac{1}{2} \nabla \times \langle \mathbf{u}_m \rangle = \Omega(\phi) \frac{\mathbf{T}_0}{8\pi\mu a^3}, \tag{138}$$

where $\langle \mathbf{\Omega} \rangle^P$ is the average particle angular velocity, $\langle \mathbf{u}_m \rangle$ is the mixture volumetric flux, $\Omega(\phi)$ is the hindrance function for rotation shown in Fig. 10 and fitted as a function of ϕ by expression (114), and $\mathbf{T}_0$ is the external torque applied to the particles.

An analogous relation for the translational slip velocity, however, does not hold. This quantity contains a finite-size correction proportional to $\nabla^2 \langle \mathbf{u}_m \rangle$, just as in the case of the familiar Faxén law for a single particle,

$$\langle \mathbf{U} \rangle^P - \langle \mathbf{u}_m \rangle = C(\phi) a^2 \nabla^2 \langle \mathbf{u}_m \rangle + U(\phi) \frac{\mathbf{F}_0}{6\pi\mu a}, \tag{139}$$

in which $\langle \mathbf{U} \rangle^P$ is the mean particle translational velocity, $U(\phi)$ is the (translational) hindrance function, and $\mathbf{F}_0$ the external force applied to the particles. The dependence of coefficient $C(\phi)$ on the volume fraction is shown in Fig. 9 and, within our numerical accuracy, is consistent with the usual value of 1/6 as the particle volume fraction tends toward zero.

The results (138) and (139) represent generalizations of the single-particle Faxén laws of Stokes flow to a spatially nonuniform suspension. The spatial nonuniformity that we have included in our study is limited to the particle number density, i.e., the one-body distribution function.

ACKNOWLEDGMENT

The authors wish to acknowledge support by DOE under Grant No. DE-FG02-99ER14966.

APPENDIX: DEFINITIONS FOR THE GENERALIZED MOBILITY PROBLEM

The generalized mobility equation, (52), is derived from the integral equation (57).

The velocity and force moments are defined by

$$\mathcal{U}^{(n)}_{i,k\ldots}(\alpha) = \frac{1}{4\pi a^2} \int_{S^\alpha} dS(\mathbf{y}) (\mathbf{y} - \mathbf{x}^\alpha)^n_{k\ldots} u_i(\mathbf{y}), \tag{A1}$$

$$\mathcal{F}^{(n)}_{j,k\ldots}(\alpha) = -\int_{S^\alpha} dS(\mathbf{y}) (\mathbf{y} - \mathbf{x}^\alpha)^n_{k\ldots} f_j(\mathbf{y}). \tag{A2}$$

$\mathbf{E}^\infty$ and $\mathcal{U}^\infty$ are defined in terms of $\mathbf{u}^\infty(\mathbf{x})$ by

$$\mathbf{E}^\infty(\alpha) = \frac{1}{4\pi a^2} \int_{S^\alpha} dS(\mathbf{y}) \frac{3}{2a^2} [(\mathbf{y} - \mathbf{x}^\alpha) \mathbf{u}^\infty(\mathbf{y}) + \mathbf{u}^\infty(\mathbf{y})(\mathbf{y} - \mathbf{x}^\alpha)], \tag{A3}$$

$$\mathcal{U}^{\infty(n)}(\alpha) = \frac{1}{4\pi a^2} \int_{S^\alpha} dS(\mathbf{y}) (\mathbf{y} - \mathbf{x}^\alpha)^n \mathbf{u}^\infty(\mathbf{y}). \tag{A4}$$

Corresponding expressions for $\mathbf{U}^\infty$ and $\mathbf{\Omega}^\infty$ were presented earlier in (53) and (54).

If, as in the cases considered in this paper, the flow imposed is given by

$$\mathbf{u}^\infty(\mathbf{x}) = \mathbf{U}^0 + \mathbf{\Omega}^0 \times \mathbf{x} + \mathbf{E}^0 \cdot \mathbf{x}, \tag{A5}$$

then,

$$\mathbf{U}^\infty(\alpha) = \mathbf{U}^0 + \mathbf{\Omega}^0 \times \mathbf{x}^\alpha + \mathbf{E}^0 \cdot \mathbf{x}^\alpha, \tag{A6}$$

$$\mathbf{\Omega}^\infty(\alpha) = \mathbf{\Omega}^0, \tag{A7}$$

$$\mathbf{E}^{\infty}(\alpha)=\mathbf{E}^{0}, \tag{A8}$$

$$\mathcal{U}^{\infty}(\alpha)=0. \tag{A9}$$

[1] G. K. Batchelor, ''Sedimentation in a dilute dispersion of spheres,'' J. Fluid Mech. **52**, 245 (1972).
[2] G. K. Batchelor and J. T. Green, ''The determination of the bulk stress in a suspension of spherical particles to order c^2,'' J. Fluid Mech. **56**, 401 (1972).
[3] H. Brenner, ''Suspension rheology in the presence of rotary Brownian motion and external couples: Elongational flow of dilute suspensions,'' Chem. Eng. Sci. **27**, 1069 (1972).
[4] M. Zuzovsky, P. M. Adler, and H. Brenner, ''Spatially periodic suspensions of convex particles in linear shear flows. III. Dilute arrays of spheres suspended in Newtonian fluids,'' Phys. Fluids **26**, 1714 (1983).
[5] H. Brenner, ''Antisymmetric stress induced by the rigid-body rotation of dipolar suspensions,'' Int. J. Eng. Sci. **22**, 645 (1984).
[6] P. Mazur, ''On the motion and Brownian motion of n spheres in a viscous fluid,'' Physica A **110**, 128 (1982).
[7] P. Mazur and W. van Saarlos, ''Many-sphere hydrodynamic interactions and mobilities in a suspension,'' Physica A **115**, 21 (1982).
[8] J. F. Brady and G. Bossis, ''Stokesian dynamics,'' Annu. Rev. Fluid Mech. **20**, 111 (1988).
[9] A. S. Sangani and A. Acrivos, ''Slow flow through a periodic array of spheres,'' Int. J. Multiphase Flow **8**, 343 (1982).
[10] A. J. C. Ladd, ''Hydrodynamic transport coefficients of random dispersions of hard spheres,'' J. Chem. Phys. **93**, 3484 (1990).
[11] A. J. C. Ladd, ''Sedimentation of homogeneous suspensions of non-Brownian spheres,'' Phys. Fluids **9**, 491 (1997).
[12] A. S. Sangani and G. Mo, ''An $O(N)$ algorithm for Stokes and Laplace interactions of particles,'' Phys. Fluids **8**, 1990 (1996).
[13] A. Sierou and J. F. Brady, ''Accelerated Stokesian dynamics simulations,'' J. Fluid Mech. **448**, 115 (2001).
[14] C. C. Chang and R. L. Powell, ''The rheology of bimodal hard-sphere dispersions,'' Phys. Fluids **6**, 1628 (1994).
[15] R. J. Phillips, J. F. Brady, and G. Bossis, ''Hydrodynamic transport properties of hard-sphere dispersions. I. Suspensions of freely mobile particles,'' Phys. Fluids **31**, 3462 (1988).
[16] J. F. Brady and L. Durlofsky, ''The sedimentation rate of disordered suspensions,'' Phys. Fluids **31**, 717 (1988).
[17] P. R. Nott and J. F. Brady, ''Pressure-driven flow of suspensions: Simulation and theory,'' J. Fluid Mech. **275**, 157 (1994).
[18] J. F. Morris and J. F. Brady, ''Pressure-driven flow of a suspension: Buoyancy effects,'' Int. J. Multiphase Flow **24**, 105 (1998).
[19] M. P. Brenner, ''Screening mechanisms in sedimentation,'' Phys. Fluids **11**, 754 (1999).
[20] F. Feuillebois, ''Sedimentation in a dispersion with vertical inhomogeneities,'' J. Fluid Mech. **139**, 145 (1984).
[21] D. Lhuillier, ''Ensemble averaging in slightly non-uniform suspensions,'' Eur. J. Mech. B/Fluids **11**, 649 (1992).
[22] M. Marchioro, M. Tanksley, W. Wang, and A. Prosperetti, ''Flow of spatially non-uniform suspensions. Part II: Systematic derivation of closure relations,'' Int. J. Multiphase Flow **27**, 237 (2001).
[23] D. Leighton and A. Acrivos, ''The shear-induced migration of particles in concentrated suspensions,'' J. Fluid Mech. **181**, 415 (1987).
[24] M. Marchioro and A. Acrivos, ''Shear-induced particle diffusivities from numerical simulations,'' J. Fluid Mech. **443**, 101 (2001).
[25] J. H. C. Luke, ''Decay of velocity fluctuations in a stably stratified suspension,'' Phys. Fluids **12**, 1619 (2000).
[26] P. N. Segré, F. Liu, P. Umbanhovar, and D. A. Weitz, ''An effective gravitational temperature for sedimentation,'' Nature (London) **409**, 594 (2001).
[27] M. Marchioro, M. Tanksley, and A. Prosperetti, ''Flow of spatially non-uniform suspensions. Part I: Phenomenology,'' Int. J. Multiphase Flow **26**, 783 (2000).
[28] W. Wang and A. Prosperetti, ''Flow of spatially non-uniform suspensions. Part III: Closure relations for porous media and spinning particles,'' Int. J. Multiphase Flow **27**, 1627 (2001).
[29] M. Tanksley and A. Prosperetti, ''Average pressure and velocity fields in non-uniform suspensions of spheres in Stokes flow,'' J. Eng. Math. **41**, 275 (2001).
[30] J. F. Brady, R. J. Phillips, J. C. Lester, and G. Bossis, ''Dynamic simulation of hydrodynamically interacting suspensions,'' J. Fluid Mech. **195**, 257 (1988).
[31] G. Mo and A. S. Sangani, ''A method for computing Stokes flow interactions among spherical objects and its application to suspensions of drops and porous particles,'' Phys. Fluids **6**, 1637 (1994).
[32] K. Ichiki, ''Improvement of the Stokesian dynamics method for systems with finite number of particles,'' J. Fluid Mech. **452**, 231 (2002).
[33] J. Happel and H. Brenner, *Low-Reynolds Number Hydrodynamics* (Prentice–Hall, Englewood Cliffs, NJ, 1965).
[34] S. Kim and S. J. Karrila, *Microhydrodynamics* (Butterworth–Heinemann, Boston, 1991).
[35] O. A. Ladyzhenskaya, *The Mathematical Theory of Viscous Incompressible Flow*, 2nd ed. (Gordon and Breach, New York, 1969).
[36] C. Pozrikidis, *Boundary Integral and Singularity Methods for Linearized Viscous Flow* (Cambridge University Press, Cambridge, 1992).
[37] H. Hasimoto, ''On the periodic fundamental solutions of the Stokes equations and their application to viscous flow past a cubic array of spheres,'' J. Fluid Mech. **5**, 317 (1959).
[38] J. K. Percus and G. J. Yevick, ''Analysis of classical statistical mechanics by means of collective coordinates,'' Phys. Rev. **110**, 1 (1958).
[39] M. S. Wertheim, ''Exact solution of the Percus–Yevick integral equation for hard spheres,'' Phys. Rev. Lett. **10**, 321 (1963).
[40] E. Thiele, ''Equation of state for hard spheres,'' J. Chem. Phys. **39**, 474 (1963).
[41] P. G. Saffman, ''On the settling speed of free and fixed suspensions,'' Stud. Appl. Math. **52**, 115 (1973).
[42] U. Geigenmüller and P. Mazur, ''Sedimentation of homogeneous suspensions in finite vessels,'' J. Stat. Phys. **53**, 137 (1988).